

PCCP

Accepted Manuscript



This is an *Accepted Manuscript*, which has been through the Royal Society of Chemistry peer review process and has been accepted for publication.

Accepted Manuscripts are published online shortly after acceptance, before technical editing, formatting and proof reading. Using this free service, authors can make their results available to the community, in citable form, before we publish the edited article. We will replace this *Accepted Manuscript* with the edited and formatted *Advance Article* as soon as it is available.

You can find more information about *Accepted Manuscripts* in the [Information for Authors](#).

Please note that technical editing may introduce minor changes to the text and/or graphics, which may alter content. The journal's standard [Terms & Conditions](#) and the [Ethical guidelines](#) still apply. In no event shall the Royal Society of Chemistry be held responsible for any errors or omissions in this *Accepted Manuscript* or any consequences arising from the use of any information it contains.

ARTICLE

Slow Dynamics of Water Confined in Newton Black Films

Cite this: DOI: 10.1039/x0xx00000x

Meng Chen,^a Xiancai Lu,^{*a} Xiandong Liu,^a Qingfeng Hou,^b Youyi Zhu,^b Huiqun Zhou^aReceived 00th January 2012,
Accepted 00th January 2012

DOI: 10.1039/x0xx00000x

www.rsc.org/

Translational and reorientational dynamics slowdowns of water confined in Newton black films (NBF) are revealed by molecular dynamics simulations. As a film becomes thinner, both translational and reorientational dynamics become slower. The polarization of water molecules in the macroscopic electrostatic field across the NBF and the coordination of Na⁺ ions and surfactant anionic groups around water molecules concertedly lead to water dynamics slowdown. The polarization effect is obvious for water not coordinated by Na⁺ ions, which exhibits reorientational dynamics depending on initial dipole orientations. Na⁺ ions and surfactant anionic groups retard dynamics of surrounding water through decreasing the hydrogen bond exchange probability and increasing the viscosity of water. The dependences of translational and reorientational dynamics on coordination environments of water are similar. Dynamics of water in positions close to the interfaces of NBFs are mainly retarded by Na⁺ ions and surfactant anionic groups, while the macroscopic polarization effect becomes the main role in influencing water dynamics in positions far from the interfaces. This study sheds light in improving knowledge about water dynamics slowdown mechanism in similar environments like reverse micelles and lamellar structures.

1. Introduction

The aqueous film sandwiched by two monolayers of amphiphilic molecules is a major constituent of foam, emulsion and some biological membrane. As the film becomes ultrathin, it loses the ability to reflect light and appears black. According to the film thickness, the black films can be classified into common black films (CBF) with 10 – 100 nm thickness and Newton black films (NBF) with < 5 nm thickness. The NBF shows strong repulsive force between two amphiphilic monolayers, which is unexpected in the Derjaguin, Landau, Verwey, and Overbeek (DLVO) theory.¹ This non-DLVO force, often called “hydration force”,^{2,3} plays an important role in maintaining the stability of films. Structures of NBFs have been well studied by experiments⁴⁻⁶ and molecular dynamics (MD) simulations.⁷⁻¹³ As shown in experiments⁶ and MD simulations,^{9, 13} dipole orientations of water preferentially point towards the anionic groups at the interface. As a result, water exhibits an anomalous dielectric response,^{13, 14} which is thought to be the origin of the hydration force.¹⁵ At low water content conditions, adhesion appears in a film. Water originally between adhesive layers is expelled forming a droplet inside the film.^{11, 12} The unusual hydration force and adhesive behavior of NBFs are inherently correlated to the solvation of ionic groups in water. Water in the hydration layer of ionic groups not only exhibits special structure, but also dynamics behaviors, *i.e.*, slower reorientational and translational motions of water.¹⁶ Water dynamics slowdowns have been found around proteins^{16, 17} and hydrophobic groups,¹⁸

beside surfactant monolayers¹⁹⁻²¹ and micellar surfaces,²²⁻²⁴ inside reverse micelles^{25, 26} and between solid surfaces.^{27, 28} Water dynamics in the hydration layer affects dynamics of proteins solvated in water,²⁹⁻³¹ and is correlated to the association of proteins.¹⁶ Similarly, the dynamics of amphiphilic molecules at the interface of a film and the adhesion of a NBF should be correlated to water dynamics. MD simulations have showed the correlation between dynamics of water and amphiphilic molecules in a NBF, revealing it to be film thickness-dependent.³² Dynamics of water and amphiphilic molecules are important for the film stability. Drainage and surface fluctuation lead to film thinning and rupture, but high surface elasticity and viscosity can retard this process.³³⁻³⁵ In a microscopic view, surface elasticity and viscosity are determined by the dynamics of amphiphilic molecules, and dynamics of water solvating them. So improving knowledge of water dynamics in NBFs is necessary.

Water confined in reverse micelles has some similarities to water in NBFs, as the interface is also covered by amphiphilic molecules. MD simulations revealed that water in a reverse micelle exhibits slower dynamics close to the interface than in the bulk-like core.²⁵ Similar phenomenon was later observed in experiments.²⁶ Experimental studies have compared different kinds of reverse micelles (with ionic or nonionic surfactants) finding that the interface, despite its chemical nature, plays the dominant role in determining interfacial water dynamics.³⁶⁻³⁸ Salt solvated in solution helps slow water dynamics, but its influence

is not as significant as the effect of the interface.³⁹ A comparison study on interfacial water dynamics in lamellar structures and reverse micelles showed that the geometry and nanolength scale of the confinement is of less significance and that the short-range water/interface interactions are of principal importance.⁴⁰ A two-component model consisting of a core of bulk-like water and a shell of interfacial water was successful at describing water reorientational dynamics in all the large reverse micelles and lamellar structures.^{40, 41} However, as the size of a reverse micelle decreases, dynamics of water get slower and transit from two ensembles to collective reorientation.⁴²⁻⁴⁴ In the MD study of water confined within nanoscopic hydrophilic silica pores, detailed molecular analyses showed that the two-component model is oversimplified and the interfacial water exhibits markedly heterogeneous dynamics.⁴⁵

Based on MD simulations, Laage and Hynes proposed the extended jump model to describe water reorientation,⁴⁶⁻⁴⁸ using it to study water reorientation slowdown next to a protein,⁴⁹ hydrophobic groups⁵⁰ and some ions.^{51, 52} They disclosed the quantitative mechanism of slower reorientational dynamics of water around cations and anions,⁵² which can also be utilized to explain similar phenomenon in the solvation shells of counterions and anion groups in reverse micelles.⁵³ The influence of ions and ionic groups is relatively short-ranged, only affecting water in the first hydration shell. On the other hand, the correlation between dynamics of water in the film and amphiphilic molecules at the interface³² is relatively long-ranged. It may imply a long-ranged influence due to the water polarization response to the electrostatic field of the film. Now we aim at doing a systematic investigation on water dynamics confined in NBFs, taking both local (counterions and ionic groups effects) and long-ranged (electrostatic field effect) influences into account.

The variation of water dynamics with film thickness is revealed by MD simulations in this article. Water dynamics dependence on positions in a film is also revealed. Coordination structures and orientations of water in thin and thick films are compared. The local coordination environment and macroscopic electrostatic field influences on water dynamics are exhibited. A detailed interpretation of water dynamics slowdown in NBFs is provided in this article.

2. Simulation details and analytic methodology

The NBF we studied is constituted by a water slab sandwiched by two monolayers of sodium dodecylsulfate (SDS) (Fig. 1). The simulation box is orthogonal with $L_x = L_y = 6.893$ nm. The film is sandwiched by two vacuum phases. The height of each vacuum phase is set to as large as 10 nm initially, so the interaction between two monolayers through the vacuum phase under the 3-dimensional periodic boundary condition can be ignored. 144 SDS molecules were set at the interface, leading to the area per molecule of 0.33 nm², corresponding to the X-ray reflection result.⁴ Films with water amount ranging from 8.43 nm² to 39.37 nm² (number of water molecules per area, N_w) were constructed. 10 films were simulated. The film thickness is defined as the distance between the averaged z coordinates of sulfur atoms at each interface. The relationship between film thickness and water amount is shown in Fig. 2.

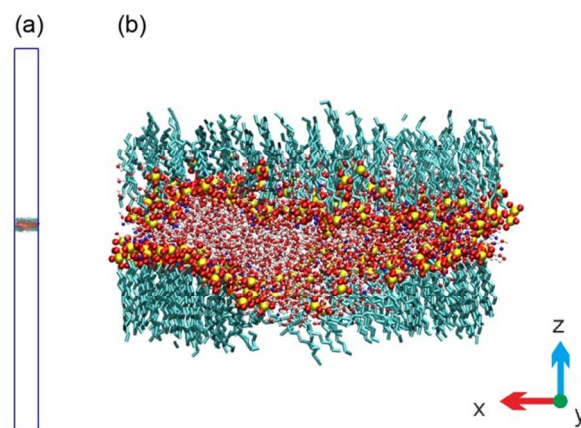


Fig. 1. (a) The model of the whole simulation box. (b) The enlarged configuration of a simulated film ($N_w = 19.68$ nm²) at 20 ns. The cyan bonds, big yellow balls, big red balls and small blue balls stand for alkyl chains, sulfur atoms, oxygen atoms and Na⁺ ions of SDS respectively. Small red balls and small white balls stand for oxygen and hydrogen atoms of water respectively. The initial configuration was built with Packmol.⁵⁴

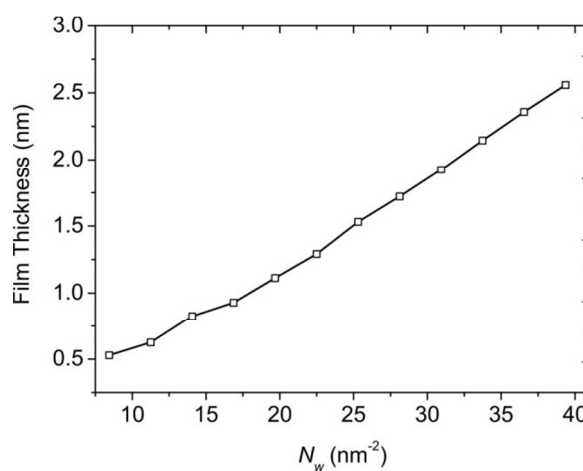


Fig. 2. Relationship between film thickness and water amount N_w . The error in calculated film thickness is less than 0.05 nm.

The SPC/E model⁵⁵ was used to describe water molecules, as it had reproduced water reorientation time consistent to experimental observables and the result of a polarizable force field.⁴⁷ The OPLS-AA force field⁵⁶ was used for SDS molecules. For bonded potential of sulfate, the force field developed by Berkowitz et al. was used.^{57, 58} Although the OPLS-AA force field was originally parameterized with the TIP3P water model,⁵⁹ the combination of the OPLS-AA force field and SPC/E model has shown to work well as compared to experimental results.^{60, 61} Especially, our previous study has shown their combination well reproduces phase structures of amphiphilic monolayers.⁶² The LINCS algorithm⁶³ was used to constrain bonds with hydrogen atoms. The cutoff distance for Lennard-Jones potential was set to 1.6 nm. The particle-mesh

Ewald (PME) method^{64, 65} was used to describe long-ranged electrostatic interactions.

The GROMACS 4.0 package⁶⁶⁻⁶⁹ was used to perform simulations in canonical ensemble (NVT) with temperature 298 K. The velocity rescaling thermostat⁷⁰ was used to control temperature. The equations of motion were integrated with a time step of 1.0 fs. MD simulations were performed for 20 ns to equilibrate systems and prolonged to 30 ns for properties evaluation. Data were collected every 1 ps. After the NVT simulations, microcanonical ensemble (NVE) simulations were performed for 200 ps for films with thicknesses 1.1 nm and 2.1 nm, collecting data every 0.05 ps. The NVE simulations served as two purposes: 1. verifying the temperature coupling method used in the NVT simulations hardly influences water dynamics (see Section A in the *Supplementary Information*); 2. studying the hydrogen bond exchange process which needs data collected between shorter time intervals.

Artificially, we define a middle layer of water centered in the middle of a film. The thickness of the layer is 0.2 nm. Dynamics of water in these layers of all the simulated films were studied. Two films with thicknesses 1.1 nm and 2.1 nm were selected to do systematic investigations for comparison. The reason for choosing these two thicknesses will be illustrated in Section 3.1. Fig. 3 shows the density profiles of the two films. Artificial layers (S_1 , S_2 , I_1 , I_2 and M) with thicknesses of 0.2 nm are marked in the density profiles, for the purpose of studying the influences of relative positions in a film to water dynamics. It should be noted that the layers are specified based on the averaged density. Due to the capillary wave fluctuation of the interfaces,^{71, 72} the distances from different locations of a layer to the interface are different, and they would vary with time. Nevertheless, the relative positions of different layers still make sense, and the differences of water dynamics among them are qualitatively meaningful.

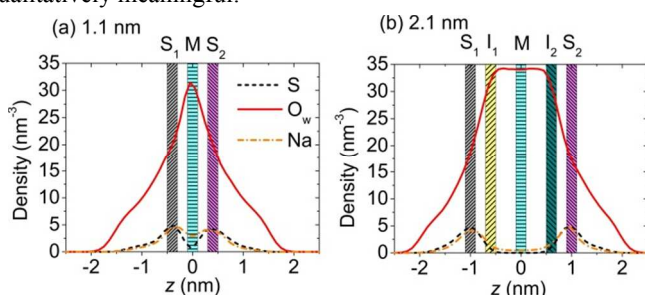


Fig. 3. Density profiles (sulfur atoms, oxygen atoms of water and Na^+ ions) of films with thicknesses 1.1 nm (a) and 2.1 nm (b). The layers (S_1 , M , I_1 ...) for water dynamics studies are marked in the profiles. “ S_1 ” and “ S_2 ” represent the two water layers at the vicinity of sulfate groups. “ M ” is marked for the water layer in the middle of the film. “ I_1 ” and “ I_2 ” denote the intermediate layers between the M layer and the S layer.

A pure water slab without surfactant with thickness about 3 nm was also simulated with the same methods for comparison. This water slab is in the same environment as NBFs because it is also sandwiched by vacuum phases. The dynamics of water from the middle 0.2 nm layer is studied. As the middle layer is far from surface, water from it behaves like bulk water.

Water dynamics are characterized by the reorientational and translational dynamics. The reorientational dynamics of water is characterized by the dipole reorientational time correlation function $C_\mu(t)$:

$$C_\mu(t) = \langle \mu_i(\tau + t) \cdot \mu_i(\tau) \rangle \quad (1)$$

where $\mu_i(\tau)$ refers to the unit vector in the dipole orientation direction of water molecule i at time τ and t is the time interval. The angular bracket denotes averaging over water molecules from all time τ . $C_\mu(t)$ was calculated for water molecules which initially belong to specific layers of the films, *i.e.*, water molecules were in that layer at time τ , but they might migrate away at time $\tau + t$. This convention has been utilized in the study of water inside reverse micelles.^{25, 53, 73} It should be noticed there has been a second convention calculating $C_\mu(t)$ only accounting for water staying in a specific region from τ to $\tau + t$.^{22, 74, 75} This convention is meaningful for studying water long confined in a specific region excluding the influence of water migrating out of that region. However, in our study, the layers specified in a system are not such confining regions, only serving as a purpose to reveal initial environmental influences to water dynamics. The reorientations of water staying and leaving the initial environment should be both taken into account. So we follow the first convention in the main text of this article. In this convention, if water molecules easily migrate out of the initial environment, it is expected $C_\mu(t)$ would exhibit a fast decay. The comparison between dynamics behaviors derived by the two conventions respectively can be seen in Section B of the *Supplementary Information*.

As to explicitly reveal the migrating ability of water in NBFs, the translational dynamics of water were also studied. Mean square displacements (MSD) of water are used to characterize the translational dynamics. Due to confinement of the film, MSD in the z direction grows nonlinearly with time, and reaches a plateau of $L^2/12$ (L is confinement size) as $t \rightarrow \infty$.⁷ At the short time scale, water diffusions in the z direction and xy plane undergo similar Brownian motions with a coefficient dependent on initial environment. At the long time scale, as water leaves initial environments and almost travels over the confining space, the diffusion coefficient becomes independent of the initial environment.⁷⁶ Thus in this article we only show the MSD of water in the xy plane ($\text{MSD}_{xy}(t)$) in less than 30 ps as for studying the initial environments influences. The Einstein relation describes the $\text{MSD}_{xy}(t)$ as:

$$\langle (x(\tau + t) - x(\tau))^2 + (y(\tau + t) - y(\tau))^2 \rangle = 4Dt \quad (2)$$

where D is the diffusion coefficient.

3. Results and discussion

3.1 Slow dynamics of water in NBFs

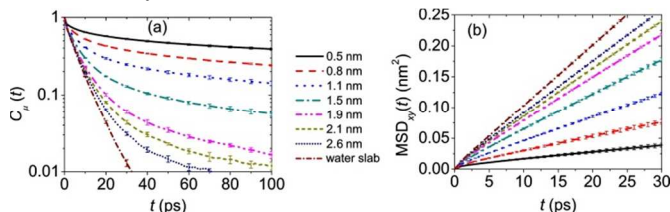


Fig. 4. $C_\mu(t)$ (a) and $\text{MSD}_{xy}(t)$ (b) of water from the middle layers of films with different thicknesses and from the pure water slab.

$C_\mu(t)$ of bulk water decays almost exponentially with time except the libration motion which occurs in subpicosecond,⁴⁸ so as that of water from the pure water slab we study. As compared to that from the pure water slab, $C_\mu(t)$ of water from the middle layers of NBFs decay slower and non-exponentially. The decay rate decreases as the film thickness decreases from 2.6 nm to 0.5 nm (Fig. 4a). As shown by $\text{MSD}_{xy}(t)$ (Fig. 4b), the translational dynamics of water in the NBF is also slower than that from the pure water slab, and becomes much slower as the film thickness decreases.

As to quantify the decay rate of $C_\mu(t)$, it is fitted with a multiexponential form function $C_\mu(t) = \sum_{i=1}^n A_i \exp(-t/\tau_i)$ (Table S1 in the *Supplementary Information*). The time constant τ_μ ($\tau_\mu = \sum_{i=1}^n A_i \tau_i$) is used to characterize the decay time.²³ τ_μ increases as the film thickness decreases (Fig. 5a). The diffusion coefficient D is used to quantify the translational motion. The characteristic residence time τ_{res} for water molecules crossing specific layer with thickness R is determined by D through the equation: $\tau_{\text{res}} = R^2/(2D)$.^{29, 77} So D^{-1} is a quantitative measurement related to water residence time in specific environment. D^{-1} also increases as the film thickness decreases (Fig. 5b).

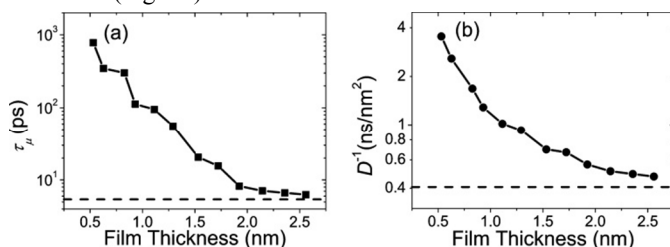


Fig. 5. Dependences of τ_μ (a) and D^{-1} (b) of water from the middle layers on film thickness. τ_μ and D^{-1} of water from the pure water slab are also shown by broken lines.

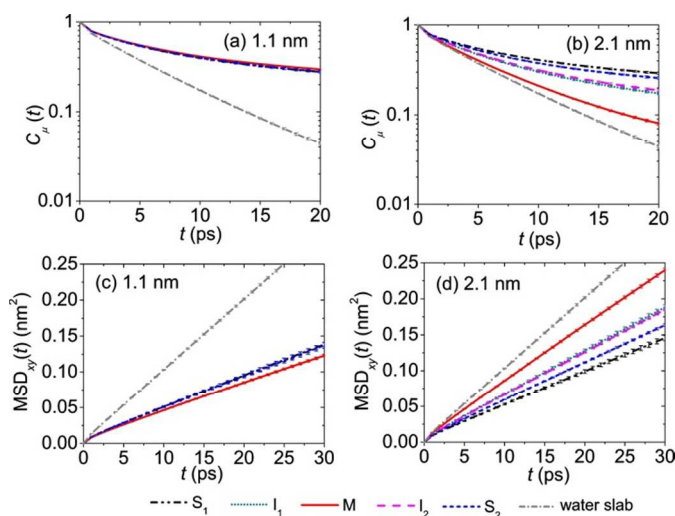


Fig. 6. $C_\mu(t)$ (a, b) and $\text{MSD}_{xy}(t)$ (c, d) of water from different layers of films with thicknesses 1.1 nm (a, c) and 2.1 nm (b, d) and from the pure water slab.

As the film thickness is above 2.0 nm, it is clear that the variations of τ_μ and D^{-1} with film thickness are relatively gentle. On the other hand, τ_μ and D^{-1} increase dramatically as the film thickness decreases more or less below 1.5 nm (Fig. 5). So a comparison study between films with thicknesses 1.1 nm and 2.1 nm has been carried out. Reorientational dynamics of water in the film with thickness 1.1 nm seem to be homogeneous, as $C_\mu(t)$ of the three layers (S_1 , M and S_2) are almost the same (Fig. 6a). $\text{MSD}_{xy}(t)$ of the three layers are also similar, except the translational motion of water in the M layer is a little slower (Fig. 6c). Both reorientational and translational motions of water from the three layers are much slower than those from the pure water slab. This phenomenon is similar to the homogeneous slow dynamics of water inside a small reverse micelle.^{42, 43} In the film with thickness 2.1 nm, $C_\mu(t)$ of S_1 and S_2 layers decay with similar rates as those in the film with thickness 1.1 nm (Fig. 6b). $C_\mu(t)$ of I_1 and I_2 layers decay slightly faster than those of S layers. $C_\mu(t)$ of the M layer decays fastest, but it still behaves non-exponentially and the decay rate is slower than that from the pure water slab. The translational dynamics are also not uniform in different layers (Fig. 6d). Water in the M layer exhibits the fastest translational motion, but it is still slower than that from the pure water slab. The translational motions in S_1 and S_2 layers are slowest, and the $\text{MSD}_{xy}(t)$ of them are similar to those in the film with thickness 1.1 nm. There is slight difference between $\text{MSD}_{xy}(t)$ of S_1 and S_2 layers, which might be caused by the asymmetry of the film due to the finite sampling. The position dependent dynamics behavior is also observed for water inside a big reverse micelle⁹ and beside a surfactant monolayer.¹⁹⁻²¹

Based on the above analyses, water dynamics transform from non-uniform dynamics along the z axis to apparent homogenous dynamics as the film thickness decreases. Previous studies have shown that the dynamics and fluctuations of the two interfaces become more correlated as the film thickness decreases.^{11, 32} So it is expected water dynamics in the thin film are influenced by both interfaces.

3.2 Structures of water confined in NBFs

The structures of water in the NBF can be characterized by the local coordination structure, and polarization structure in the electrostatic field of the film. The coordination structure of a water molecule was determined according to the hydrogen bonds (HB) formed between it and surrounding water molecules and/or sulfate groups. The HB definition can be seen in Section D of the *Supplementary Information*. In this article, the coordination modes are represented by “ $O_iH_jH_k$ ”, “ $O_iH_jH'k$ ” and “ $O_iH'_jH'k$ ”. “ $O_iH_jH_k$ ” represents that the oxygen atom of the water molecule accepts i HBs, and either hydrogen atom forms j or k HBs with other water molecules. As to “ $O_iH_jH'k$ ”, one hydrogen atom forms j HBs with other water molecules, and the other one forms k HBs with sulfate groups. As to “ $O_iH'_jH'k$ ”, either hydrogen atom forms j or k HBs with sulfate groups. Comparisons of the probability distributions of coordination modes among water from films with thicknesses 1.1 nm and 2.1 nm and from the pure water slab are described in Section D of the *Supplementary Information*. Three characteristic coordination modes (“ $O2H1H1$ ”, “ $O0H1H1$ ”, and “ $O2H1H'1$ ”) are found through snapshots of simulations (Fig. 7). The coordination mode “ $O2H1H1$ ” exhibiting a tetrahedral structure (Fig. 7a), is the

most popular structure in films and the pure water slab. Water accepting no HB like “O0H1H1” rarely exists in the pure water slab, but it appears in quantity in films. As shown in the snapshot, the O atom of that kind of water molecules in films closely interacts with a Na⁺ ion (Fig. 7b). Water accepting only one HB (“O1H0H1”, “O1H1H1” and so on) appears both in films and the pure water slab. Water donating some HB to a sulfate group like “O2H1H1” (Fig. 7c) appears in water layers close to the SDS monolayers. Detailed characterizations on the Na⁺-water relation are shown in Section E of the *Supplementary Information*. It clearly shows that water accepting no HB (like “O0H1H1” and “O0H0H1”) has the closest relationship with Na⁺ ions. A water molecule of that kind is mostly coordinated by a Na⁺ ion stably as in Fig. 7b. About half of the water molecules accepting only one HB (like “O1H0H1” and “O1H1H1”) are coordinated by a Na⁺ ion. Water molecules accepting two HBs (like “O2H0H1” and “O2H1H1”) are rarely coordinated by Na⁺ ions.

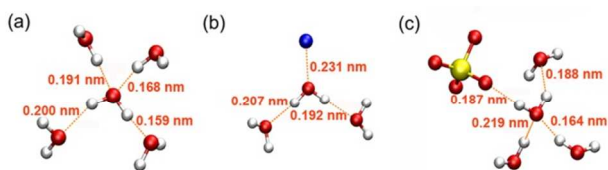


Fig. 7. Coordination structures of modes “O2H1H1” (a), “O0H1H1” (b) and “O2H0H1” (c). The red balls stand for oxygen atoms, white balls for hydrogen atoms, yellow balls for sulfur atoms and blue balls for Na⁺ ions.

Due to the polarization, dipoles of water molecules prefer to point towards the interface, exhibiting long-ranged ordered structure.^{9, 13, 14} The electrostatic fields across the films and the polarizations of water molecules are shown in Section F of the *Supplementary Information*. Water molecules across the films are all under polarization effects. The polarization of water molecules in the electrostatic field is characterized by the tilt angle (θ), which is the angle between the dipole moment of water and the z axis. θ of higher probabilities correspond to more favored polarized directions. Fig. 8 exhibits the distributions of θ in different layers of the two films. In either film, the distributions are sharpest in the S layers, reflecting the most obvious polarized structures. In the I layers, the distributions are gentler, as these layers are farther to the interfaces. It is clear that water in the M layer of the film with thickness 1.1 nm is polarized by both interfaces (Fig. 8a). Even water in the M layer of the film with thickness 2.1 nm still exhibits slight polarized structure (Fig. 8b).

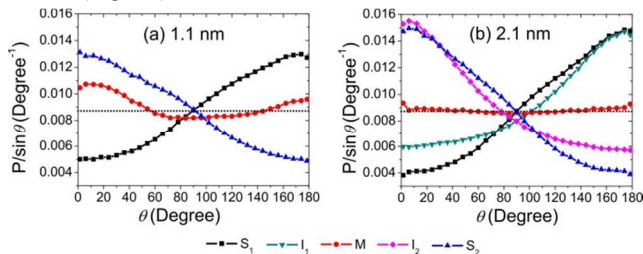


Fig. 8. Distributions of tilt angle θ of water in different layers of films with thicknesses 1.1 nm (a) and 2.1 nm (b). The distributions are normalized by $\sin \theta$. The dotted line shows the theoretical distribution of bulk water.

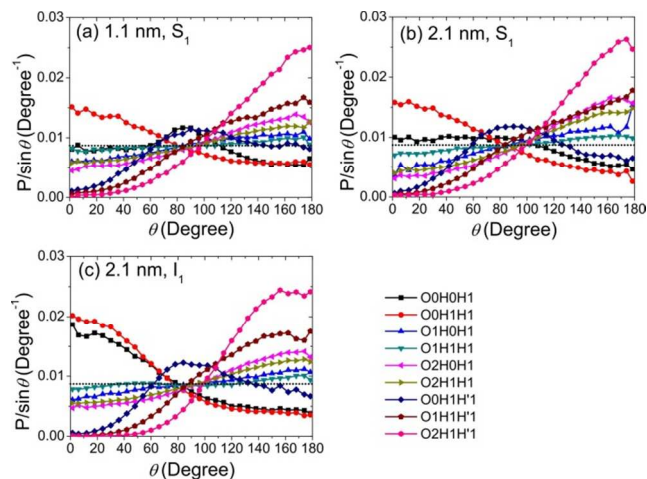


Fig. 9. Tilt angle distributions of water of different coordination modes in different layers of films with thicknesses 1.1 nm and 2.1 nm. The distributions are normalized by $\sin \theta$. The dotted line shows the theoretical distribution of bulk water.

The influence of the electrostatic field to the polarization is further considered independently for water molecules of different coordination modes (Fig. 9). Water in S₁ and I₁ layers is considered as its polarized structure is obvious. Dipoles of water of modes “O2H0H1” and “O2H1H1” prefer to be in the macroscopic polarized direction of the electrostatic field. Water of “O1H0H1” and “O1H1H1” exhibits the same trend, except the distributions are gentler, which are probably due to the local influence of Na⁺ ions. Water molecules of modes “O0H0H1” and “O0H1H1” exhibit different distribution trends to others, probably because they are stably coordinated by Na⁺ ions. Water molecules of “O2H1H1” exhibit the sharpest distributions in the macroscopic polarized direction, as they directly donate HBs to sulfate groups. It should be noted that the distribution does not become zero even when θ of “O2H1H1” water molecules are less than 60°. Because the sulfate groups are in fact in the aqueous phase and solvated by water and the interface is fluctuating,^{72, 78} it is possible that water molecules solvating sulfate groups exhibit dipoles in all directions. Water of “O1H1H1” exhibits less sharp distributions than that of “O2H1H1” due to the Na⁺ ions influence. Orientations of water of “O0H1H1” are both influenced by sulfate groups and Na⁺ ions, so that they do not exhibit the sharp distribution in the macroscopic polarized direction and a peak around 90° appears in the distribution.

The macroscopic polarization of water is inherently determined by the distributions of ions (surfactant anions in the monolayer and diffusive counterions Na⁺).¹⁴ So the polarization structures are strongest for water around surfactant anions and relatively weaker for water not coordinated by them. However, the Na⁺ ions also exert a large influence, polarizing nearby water molecules in spite of the macroscopic electrostatic field. The influence of Na⁺ ions is relatively short-ranged, while the

macroscopic polarization is a long-ranged influence responsible for the structure of water even in the middle of the films we studied.

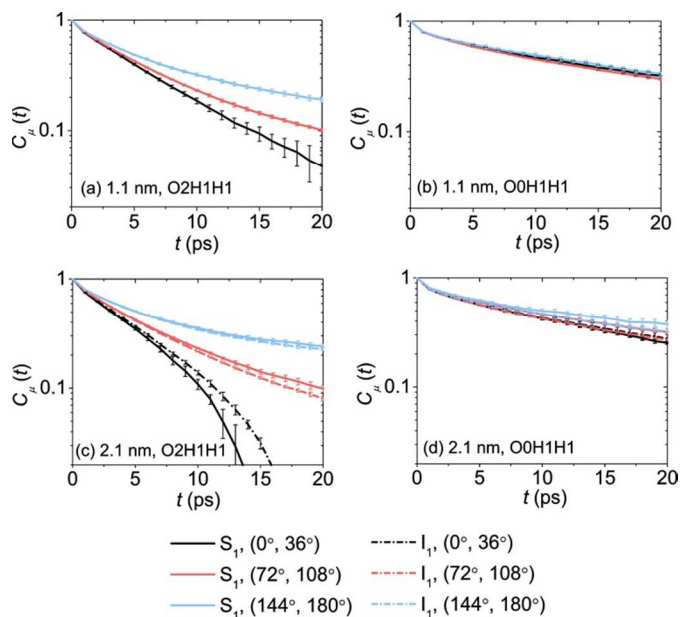


Fig. 10. The dependences of $C_\mu(t)$ on water initial tilt angles for water from different layers. Coordination modes are “O2H1H1” (a, c) and “O0H1H1” (b, d). The film thicknesses are 1.1 nm (a, b) and 2.1 nm (c, d).

3.3 Water dynamics dependence on coordination and orientation

As to study the possible influence of the macroscopic electrostatic field to water reorientational dynamics, water molecules were classified according to their initial tilt angles (θ). Fig. 10 exhibits reorientational dynamics of water with θ in ranges from 0° to 36° , from 72° to 108° and from 144° to 180° . For water molecules of coordination mode “O2H1H1” in the S_1 and I_1 layers of the film with thickness 2.1 nm, the decays of $C_\mu(t)$ strongly depend on θ (Fig. 10c). The dependence is stronger for water in the S_1 layer as it is closer to the interface. Those orientated closer to the macroscopic polarized direction (with θ between 144° and 180°) exhibit slower dynamics, and $C_\mu(t)$ of them are concave in the semilogarithmic coordinate system. While dipoles of those water molecules deviate from the original directions, they tend to reorient back to the favored polarized directions, which leads to the non-exponential decays of $C_\mu(t)$. On the other hand, for water molecules with θ in the range between 0° and 36° , $C_\mu(t)$ are convex in the studied time range. As initial orientations of those water molecules deviate from the polarized direction, they would reorient to adapt to the electrostatic field, leading to the observed dramatic variation in $C_\mu(t)$. For water molecules of coordination mode “O2H1H1” in the S_1 layer of the film with thickness 1.1 nm, $C_\mu(t)$ still depends on θ but less strongly (Fig. 10a). In that case no convex function line appears for water with θ between 144° and 180° . It implies that due to the smaller film thickness even water molecules close to one monolayer are under the polarization effect of the other

monolayer. So the reorientations of water molecules which deviate from the favored polarized direction are less dramatic. For water molecules of coordination mode “O0H1H1”, the reorientational dynamics dependence on θ is not obvious, especially in the thinner film (Fig. 10b,d).

Reorientational dynamics dependence on θ for water molecules of other coordination modes can be seen in Section G of the *Supplementary Information*. Water accepting no less than 2 HBs is significantly influenced by the macroscopic electrostatic field, exhibiting obvious θ dependent reorientational dynamics. Water accepting 1 HB exhibits weaker θ dependent reorientational dynamics. The dependence is weakest for water accepting 0 HB. That implies the local influence of Na^+ ions plays an important role, weakening the macroscopic electrostatic field effect, as Section 3.2 has shown that the Na^+ ions can polarize water in spite of the macroscopic electrostatic field.

Reorientational dynamics dependence on coordination environment is shown for water molecules originally not in the polarized directions (Fig. 11). Dynamics of water from the pure water slab are independent of coordination structures (see Section H of the *Supplementary Information*). In the M layer of the film with thickness 2.1 nm (Fig. 11c), the reorientational dynamics are similar for all the coordination modes except “O0H0H1” and “O0H1H1” which represent close relationships with Na^+ ions. $C_\mu(t)$ of “O0H0H1” and “O0H1H1” decay slower. In other situations (Fig. 11a,b,d), dynamics of water which does not form HBs with sulfate groups follow the order: O0HjHk < O1HjHk < O2HjHk, i.e., water molecules with closer relationships with Na^+ ions exhibit slower dynamics. However, the number of HBs donated by one water molecule to another almost has no influence. $C_\mu(t)$ of “O2H1H1”, “O1H1H1” and “O0H1H1” decay slower than those of “O2H1H1”, “O1H1H1” and “O0H1H1” separately, showing that water molecules donating HBs to sulfate groups exhibit slower dynamics. The influence of Na^+ ions on those water molecules is the same, as their dynamics follow the order: O0H1H1 < O1H1H1 < O2H1H1.

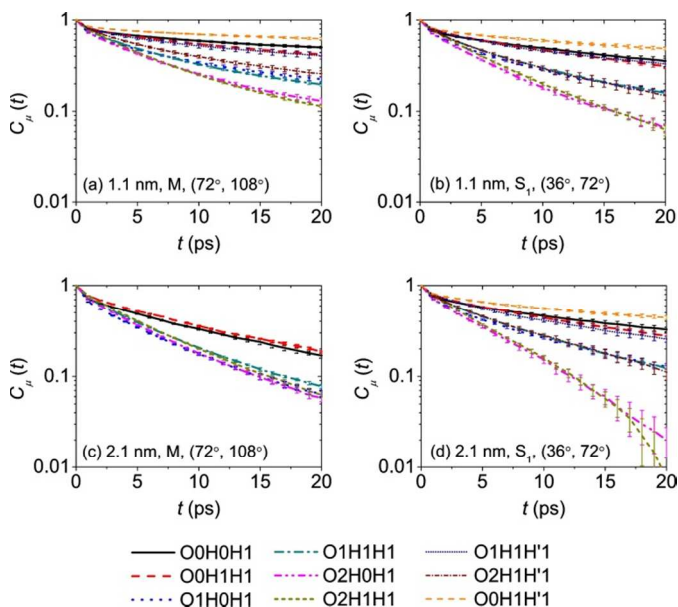


Fig. 11. The dependence of $C_\mu(t)$ on the coordination modes of water. The M and S_1 layers of films with thicknesses 1.1 nm (a, b)

and 2.1 nm (c, d) are considered. The initial tilt angles are in the ranges from 72° to 108° (a, c) and from 36° to 72° (b, d) respectively.

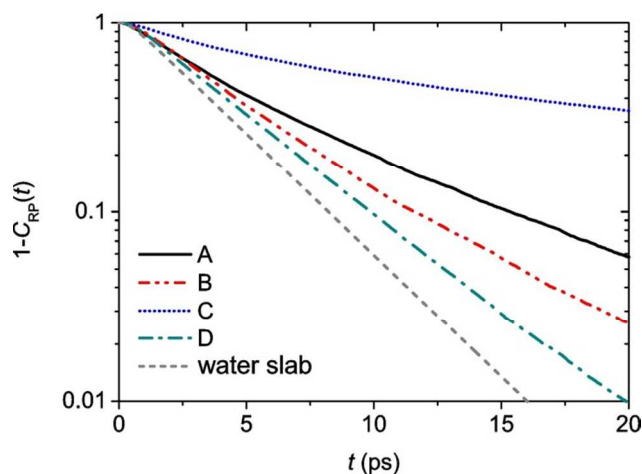


Fig. 12. Time correlation functions $1 - C_{RP}(t)$ for different kinds of water OH bonds in the S_1 layer of the film with thickness 2.1 nm. A: OH bonds which are hydrogen bonded to sulfate groups but not in the hydration shell of Na^+ ions. B: OH bonds which are in the hydration shell of Na^+ ions but not hydrogen bonded to sulfate groups. C: OH bonds both hydrogen bonded to sulfate groups and in the hydration shell of Na^+ ions. D: OH bonds neither hydrogen bonded to sulfate groups nor in the hydration shell of Na^+ ions. $1 - C_{RP}(t)$ for water from the pure water slab is also shown for comparison.

The traditional Debye model which describes water reorientations to be diffusive angular Brownian motions was in contrast to MD simulation results.^{47, 53, 74} Laage and Hynes proposed the extended jump model to describe water reorientation. The reorientation is separated into the diffusive frame reorientation between HB exchanges, and the jump reorientation while HBs exchange acceptors.⁴⁶⁻⁴⁸ With that model, the mechanisms of water reorientational dynamics slowdown in salt solutions with Na^+ and SO_4^{2-} ions are disclosed.⁵² The retardations by Na^+ and SO_4^{2-} ions in reorientational dynamics of surrounding water molecules can be attributed to two mechanisms: 1. the jump probability of an OH bond in a preformed HB to a new HB is reduced due to the volume occupied by ions and the stronger HB between a water molecule and a sulfate group; 2. the increased viscosity of water solvating the ions slows down the diffusive frame reorientation.⁵² These two mechanisms should also apply to water reorientational dynamics dependence on coordination environments. Now we disclose the influences of these two mechanisms respectively as follows.

The jump reorientation due to the HB exchange is characterized by the cross correlation function:

$$C_{RP}(t) = \langle n_R(0)n_P(t) \rangle \quad (3)$$

where $n_R(0)$ is 1 if the OH bond of a water molecule forms a stable HB with an acceptor (water molecules or sulfate groups) at time 0, $n_P(t)$ is 1 if the OH bond forms a new stable HB with another acceptor at time t , otherwise their values are 0. As to

define a stable HB, a strict geometric definition should be used.⁴⁷ The definition we used is as follows: the donor-accepter distance, the hydrogen-donor-accepter angle, and the hydrogen-accepter distance are less than 0.28 nm, 10° , and 0.18 nm respectively. The decay of the time correlation function $1 - C_{RP}(t)$ reflects the HB exchange rate, in other words, the residential time of a water OH bond in its initial coordination environment. OH bonds both hydrogen bonded to sulfate groups and in the hydration shell of Na^+ ions exhibit the slowest HB exchange rate (Fig. 12). Either OH bonds donating HBs to sulfate groups or in the hydration shell of Na^+ ions exhibit slower HB exchanges than those of water not coordinated by ions. This result is consistent with the dependence of $C_\mu(t)$ on the coordination modes of water, *i.e.*, water molecules in closer relationships with Na^+ ions and sulfate groups exhibit slower reorientational dynamics (Fig. 11). So the retardation by ions in the HB exchange contributes to water reorientational dynamics slowdown.

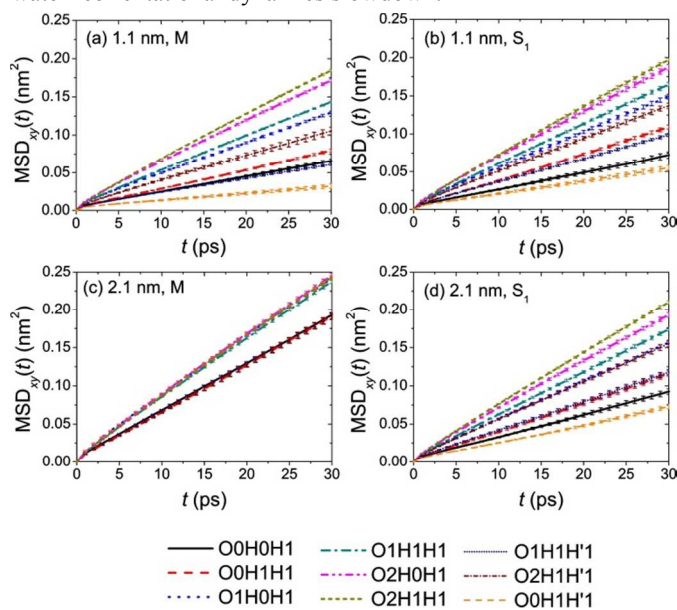


Fig. 13. The dependences of $\text{MSD}_{xy}(t)$ on the coordination modes of water. The M and S_1 layers of films with thicknesses 1.1 nm (a, b) and 2.1 nm (c, d) are considered.

The HB jump exchange induces a translational displacement of water. Based on the Stokes-Einstein relation, the translational dynamics is in inverse relationship with the viscosity η . η is related to the HB jump time constant τ_{jump} with a qualitative relation: $\tau_{jump}/L^2 \propto \eta$, where L is the translational jump amplitude.^{52, 79} On the other hand, the viscosity also influences the diffusive frame reorientation of water with a qualitative relation: $\eta \propto \tau_{frame}$, where τ_{frame} is the frame reorientation time constant of water.⁵² So the translational dynamics is closely related to the reorientational dynamics. The translational dynamics dependence on water coordination was studied and similarities as the reorientational dynamics are disclosed (Fig. 13). In layers largely influenced by the interfaces (the S_1 layers of the two films and the M layer of the thinner film, Fig. 13a,b,d), the translational dynamics for water which does not form HBs with sulfate groups follow the same order as the reorientational dynamics: $\text{O0HjHk} < \text{O1HjHk} < \text{O2HjHk}$. The translational dynamics of O2H1H'1 , O1H1H'1 and O0H1H'1 are also slower

than those of O2H1H1, O1H1H1 and O0H1H1 respectively as the reorientational dynamics. And the order “O0H1H1 < O1H1H1 < O2H1H1” also applies to the translational dynamics. In the M layer of the thicker film, the translational dynamics of water of modes “O0H0H1” and “O0H1H1” are also slower than others as the reorientational dynamics (Fig. 13c). These results evidence the coupling between the reorientational and translational dynamics. This coupling relationship reflects the viscosity mechanism in slowing down water reorientational dynamics.

The above mechanisms well explain the water dynamics dependence on local coordination environments. It should be noted that these mechanisms almost have no relation with the local electrostatic field induced by ions, as Laage et. al. have shown the local electrostatic field almost has no influence on water dynamics.⁵² Our results are in consistence to it, as we have shown that even though Na⁺ ions induce regular distributions of dipole tilt angles θ for water molecules around them (Fig. 9), the reorientation of those water molecules is not obviously dependent on θ (Fig. 10). On the other hand, the long-ranged electrostatic field which is specific in the NBF has a large influence on the reorientational dynamics of water which is not coordinated by Na⁺ ions and sulfate groups (e.g. “O2H1H1”). Water molecules coordinated by sulfate groups (e.g. “O2H1H1”) also exhibit θ dependent reorientational dynamics (see Section G of the *Supplementary Information*), showing the macroscopic electrostatic field influence. However, the retardation effect of sulphate groups plays the main role as even water with dipoles deviating from the favoured polarized direction exhibits obviously slow dynamics.

The two-component model was used to describe water dynamics confined in all the large reverse micelles and lamellar structures.^{40, 41} This model is useful but oversimplified, as our study has shown that there is not a shell of interfacial water exhibiting homogeneous dynamics. Even water in the core of the thick NBF is not totally homogeneous as water coordinating diffusive Na⁺ ions exhibit slower dynamics (Fig. 11c and Fig. 13c). The different coordination relationships between water and ions (Na⁺ ions and surfactant anions) lead to the heterogeneous dynamics. Due to the polarization effect, even dynamics of water not coordinating ions (e.g. “O2H1H1”) are heterogeneous being dependent on initial dipole orientations.

3.4 Relative contributions of different kinds of water to dynamics slowdown

The overall slowdown of water reorientational dynamics is characterized by $\Delta C_\mu(t)$:

$$\Delta C_\mu(t) = \sum_i P_i [C_\mu^i(t) - C_\mu^{bulk}(t)] \quad (4)$$

where P_i and $C_\mu^i(t)$ are the proportion and dipole reorientational time correlation function of the i th kind water molecules respectively, and $C_\mu^{bulk}(t)$ is the dipole reorientational time correlation function for bulk water which is the same as $C_\mu(t)$ for water from the pure water slab. The meaning of Eq. (4) is accounting for the contributions of dynamics slowdowns of each kind of water molecules. Now water molecules in NBFs are simplified into 6 kinds: O0, O1, O2/3, O0H', O1H' and O2/3H', based on the dynamics influencing factors (macroscopic

polarization effect and retardations by Na⁺ ions and sulfate groups). “O0” characterizes water molecules which accept no HB and are largely influenced by Na⁺ ions; “O1” characterizes water molecules which accept only one HB, moderately influenced by Na⁺ ions and the macroscopic polarization effect; “O2/3” characterizes water molecules which accept 2 or 3 HBs, hardly influenced by Na⁺ ions but obviously influenced by the macroscopic polarization effect. “O0H’”, “O1H’” and “O2/3H’” characterize water molecules accepting 0, 1 and 2 or 3 HBs respectively and donating HBs to sulfate groups, and their dynamics are retarded by sulfate groups. So $\Delta C_\mu(t)$ in Eq. (4) can be separated into 6 contributions: $\Delta C_\mu^{O0}(t)$, $\Delta C_\mu^{O1}(t)$, $\Delta C_\mu^{O2/3}(t)$, $\Delta C_\mu^{O0H'}(t)$, $\Delta C_\mu^{O1H'}(t)$ and $\Delta C_\mu^{O2/3H'}(t)$.

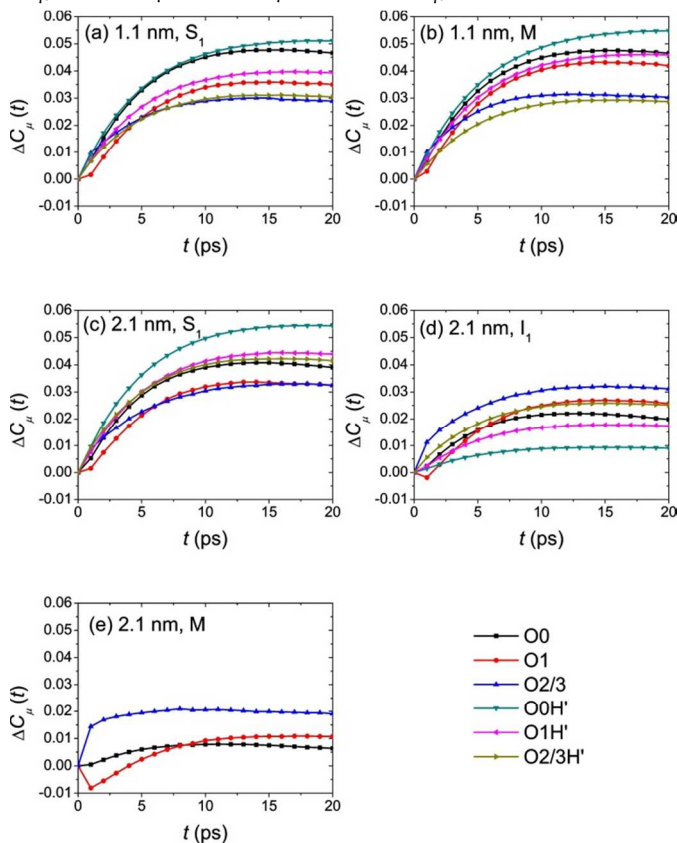


Fig. 14. Contributions of different kinds of water to $\Delta C_\mu(t)$ in different layers of films with thicknesses 1.1 nm and 2.1 nm.

Fig. 14 exhibits the 6 contributions to $\Delta C_\mu(t)$. Although water from the S₁ and M layers of the film with thickness 1.1 nm apparently exhibits similar dynamics (Fig. 6a), the individual contributions are quantitatively different (Fig. 14a,b). It implies that the mechanisms behind water dynamics slowdown are different. In those layers, the biggest contributions to water dynamics slowdowns are $\Delta C_\mu^{O0H'}(t)$. Even though the populations of “O0H’” water molecules are not so significant as compared to other kinds of water in those layers (Fig. S3 in the *Supplementary Information*), because they exhibit the slowest dynamics (Fig. 11), their contributions are strengthened. In the S₁ layer of the film with thickness 2.1 nm (Fig. 14c), the individual contributions are different from those in the S₁ layer of the

thinner film (Fig. 14a), although apparently water in the two layers exhibits similar dynamics (Fig. 6a,b). The biggest contribution is also $\Delta C_{\mu}^{OH^I}(t)$. However, in the I_1 layer of the film with thickness 2.1 nm (Fig. 14d), the contribution of $\Delta C_{\mu}^{OH^I}(t)$ decreases a lot due to much less water molecules coordinating sulfate groups and Na^+ ions in that layer. $\Delta C_{\mu}^{O2/3}(t)$ becomes the biggest contribution in that layer, *i.e.*, the influence of the macroscopic electrostatic field becomes most important to water reorientational dynamics slowdown. “O2/3” water molecules exhibit higher populations in the macroscopic polarized direction (Fig. 9) and slower reorientational dynamics in that direction (Fig. 10), leading to the overall slow dynamics. $\Delta C_{\mu}^{O2/3}(t)$ mainly determines the reorientational dynamics slowdown in the M layer of the film with thickness 2.1 nm (Fig. 14e). Although that layer is far from the interface, the macroscopic electrostatic field influence is still obvious (see Section F of the *Supplementary Information*). The retardation effect of Na^+ ions plays a minor role in water dynamics slowdown in that layer.

The macroscopic polarization effect and the retardation of Na^+ ions and sulfate groups concerted lead to the dynamics slowdown of water in NBFs. The retardation effects of ions are important to slowing down water dynamics in positions close to the interfaces. In positions farther to the interfaces, the macroscopic polarization effect is becoming the main role in influencing water dynamics.

Previous experimental studies have compared reverse micelles with ionic and nonionic surfactants at the interfaces, showing the orientational relaxations of interfacial water molecules are similar.³⁷ As analyzed in Section 3.3, the retardation effects of ions at the interface are due to the volume exclusion of ions, HBs with ions and the increased viscosity of water. Those effects are not caused by the charges of ions, and should also be present for water interacting with hydrophilic groups of nonionic surfactants at the interface. Thus it is reasonable water close to the nonionic and ionic surfactants interfaces exhibits similar dynamics. On the other hand, the long-ranged macroscopic polarization effect due to the charged interface is expected to be absent in the systems with nonionic surfactants. A detailed comparison study between NBFs with ionic and nonionic surfactants should be processed in the future.

Concluding remarks

In this study, we have used MD simulations disclosing the reorientational and translational dynamics slowdowns of water confined in NBFs. The constants τ_{μ} and D^{-1} are used to characterize the reorientational and residential time of water in the middle layer of the films. They increase gently as the film thickness decreases at first, then exhibit dramatic increment. Two films with thicknesses belonging to gently and dramatically increasing stages of τ_{μ} and D^{-1} respectively have been selected for comparisons. Apparently dynamics of water in different positions of the thinner film are similar, while water closer to the interfaces of the thicker film exhibit obviously slower dynamics.

For water molecules less affected by Na^+ ions and sulfate groups, due to the polarization in the macroscopic electrostatic field, their dynamics obviously depend on the original

orientations of their dipoles, and those orient close to the polarized direction exhibit slower dynamics. Na^+ ions and sulfate groups coordinating water retard its dynamics. The retardations are attributed to two mechanisms: firstly, the jump probability of an OH bond in a preformed HB to a new HB is reduced due to the volume occupied by ions and the stronger HB between a water molecule and a sulfate group; secondly, the increased viscosity of water solvating the ions slows down the diffusive frame reorientation. The first mechanism is verified by disclosing slower HB exchanges for water coordinated by ions. The second mechanism is exhibited by disclosing the coupling between translational and reorientational dynamics of water in the same coordination environment.

The macroscopic polarization effect and the retardation of Na^+ ions and sulfate groups concerted lead to the dynamics slowdown of water in NBFs. For water molecules in the thinner film and in the layers close to the interfaces of the thicker film, the retardation of Na^+ ions and sulfate groups plays the main role, as the concentration of Na^+ ions is high and a number of water molecules form HBs with sulfate groups. On the other hand, the macroscopic polarization effect is becoming the main role in influencing water dynamics in positions farther to the interfaces of the thicker film.

This MD simulation study has been performed with non-polarizable force fields, but the influences of ions disclosed in this study are in consistency with the expectations of experiments and simulations with polarizable force fields.³² MD simulation studies with polarizable force fields⁸⁰⁻⁸² may give quantitatively more accurate results, and are better for comparing influences of ionic and nonionic surfactants to water dynamics. This requires future studies. In addition, the analysis method in our study can also be utilized to study dynamics of water beside surfactant monolayers and micelles, and inside reverse micelles.

Acknowledgements

We acknowledge the China National Science and Technology Major Project 2011ZX05010-005 and National Basic Research Program (973) of China (No.2012CB214803). We are grateful to the High Performance Computing Center of Nanjing University for using the IBM Blade cluster system.

Notes and references

^a State Key Laboratory for Mineral Deposits Research, School of Earth Sciences and Engineering, Nanjing University, Nanjing Jiangsu, 210093, China. E-mail: xcljun@nju.edu.cn, Fax: +86-25-83686016

^b State Key Laboratory of Enhanced Oil Recovery, Research Institute of Petroleum Exploration and Development, CNPC, Beijing 100083, China.

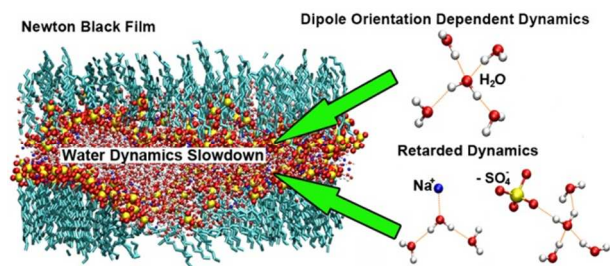
Electronic Supplementary Information (ESI) available: Comparison of water dynamics in NVT and NVE ensembles, comparison of dynamics of water originally in a specific layer and remained in a specific layer, multiexponential fitting parameters for dipole reorientational time correlation functions, coordination modes distributions of water, relation between water and Na^+ ions, electrostatic field and water orientation across the film, reorientational dynamics dependence on water orientation and reorientational dynamics of water from the pure water slab.

1. E. D. Shchukin, A. V. Pertsov, E. A. Amelina and A. S. Zelenev, *Colloid and Surface Chemistry*, Elsevier, Amsterdam, 2001.

2. S. Leikin, V. A. Parsegian, D. C. Rau and R. P. Rand, *Annu. Rev. Phys. Chem.*, 1993, **44**, 369-395.
3. E. Ruckenstein and M. Manciu, *Langmuir.*, 2002, **18**, 2727-2736.
4. O. Bèlorgey and J. Benattar, *Phys. Rev. Lett.*, 1991, **66**, 313.
5. L. Evers, E. Nijman and G. Frens, *Colloid Surface. A.*, 1999, **149**, 521-527.
6. C. Berger, B. Desbat, H. Kellay, J.-M. Turllet and D. Blaudez, *Langmuir.*, 2003, **19**, 1-5.
7. F. Bresme and J. Faraudo, *Langmuir.*, 2004, **20**, 5127-5137.
8. S. S. Jang and W. A. Goddard, *J. Phys. Chem. B*, 2006, **110**, 7992-8001.
9. F. Bresme and J. Faraudo, *Mol. Simulat.*, 2006, **32**, 1103-1112.
10. F. Bresme and E. Artacho, *J. Mater. Chem.*, 2010, **20**, 10351-10358.
11. F. Bresme, E. Chacón, H. Martínez and P. Tarazona, *J. Chem. Phys.*, 2011, **134**, 214701.
12. P. Tarazona, H. Martínez, E. Chacon and F. Bresme, *Phys. Rev. B*, 2012, **85**, 085402.
13. M. Chen, X. Lu, X. Liu, Q. Hou, Y. Zhu and H. Zhou, *J. Phys. Chem. C*, 2012, **116**, 21913-21922.
14. J. Faraudo and F. Bresme, *Phys. Rev. Lett.*, 2004, **92**, 236102.
15. J. Faraudo and F. Bresme, *Phys. Rev. Lett.*, 2005, **94**, 077802.
16. B. Bagchi, *Chem. Rev.*, 2005, **105**, 3197-3219.
17. C. Rocchi, A. R. Bizzarri and S. Cannistraro, *Phys. Rev. E*, 1998, **57**, 3315-3325.
18. Y. Rezus and H. Bakker, *Phys. Rev. Lett.*, 2007, **99**, 148301.
19. J. Chanda and S. Bandyopadhyay, *J. Chem. Theory Comput.*, 2005, **1**, 963-971.
20. J. Chanda, S. Chakraborty and S. Bandyopadhyay, *J. Phys. Chem. B*, 2005, **109**, 471-479.
21. J. Chanda and S. Bandyopadhyay, *J. Phys. Chem. B*, 2006, **110**, 23482-23488.
22. S. Balasubramanian and B. Bagchi, *J. Phys. Chem. B*, 2002, **106**, 3668-3672.
23. S. Pal, S. Balasubramanian and B. Bagchi, *J. Chem. Phys.*, 2002, **117**, 2852-2859.
24. S. Pal, S. Balasubramanian and B. Bagchi, *Phys. Rev. E*, 2003, **67**, 061502.
25. J. Faeder and B. Ladanyi, *J. Phys. Chem. B*, 2000, **104**, 1033-1046.
26. A. M. Dokter, S. Woutersen and H. J. Bakker, *Proc. Natl. Acad. Sci. U.S.A.*, 2006, **103**, 15355-15358.
27. N. Choudhury and B. M. Pettitt, *J. Phys. Chem. B*, 2005, **109**, 6422-6429.
28. S. Romero-Vargas Castrillón, N. Giovambattista, I. A. Aksay and P. G. Debenedetti, *J. Phys. Chem. B*, 2009, **113**, 7973-7976.
29. S. K. Pal, J. Peon, B. Bagchi and A. H. Zewail, *J. Phys. Chem. B*, 2002, **106**, 12376-12395.
30. B. Halle and M. Davidovic, *Proc. Natl. Acad. Sci. U.S.A.*, 2003, **100**, 12135-12140.
31. A. Mukherjee and B. Bagchi, *Chem. Phys. Lett.*, 2005, **404**, 409-413.
32. S. Di Napoli and Z. Gamba, *J. Chem. Phys.*, 2010, **132**, 075101.
33. V. Bergeron, *J. Phys.: Condens. Mat.*, 1999, **11**, R215.
34. D. Langevin, *Adv. Colloid Interface Sci.*, 2000, **88**, 209-222.
35. R. v. Klitzing and H.-J. Müller, *Curr. Opin. Colloid Interface Sci.*, 2002, **7**, 42-49.
36. D. E. Moilanen, N. E. Levinger, D. Spry and M. Fayer, *J. Am. Chem. Soc.*, 2007, **129**, 14311-14318.
37. E. E. Fenn, D. B. Wong and M. Fayer, *Proc. Natl. Acad. Sci. U.S.A.*, 2009, **106**, 15243-15248.
38. M. D. Fayer, *Accounts. Chem. Res.*, 2011, **45**, 3-14.
39. S. Park, D. E. Moilanen and M. D. Fayer, *J. Phys. Chem. B*, 2008, **112**, 5279-5290.
40. D. E. Moilanen, E. E. Fenn, D. Wong and M. Fayer, *J. Am. Chem. Soc.*, 2009, **131**, 8318-8328.
41. D. E. Moilanen, E. E. Fenn, D. Wong and M. Fayer, *J. Phys. Chem. B*, 2009, **113**, 8560-8568.
42. D. E. Moilanen, E. E. Fenn, D. Wong and M. D. Fayer, *J. Chem. Phys.*, 2009, **131**, 014704.
43. P. A. Pieniazek, Y.-S. Lin, J. Chowdhary, B. M. Ladanyi and J. Skinner, *J. Phys. Chem. B*, 2009, **113**, 15017-15028.
44. M. D. Fayer and N. E. Levinger, *Annu. Rev. Anal. Chem.*, 2010, **3**, 89-107.
45. D. Laage and W. H. Thompson, *J. Chem. Phys.*, 2012, **136**, 044513.
46. D. Laage and J. T. Hynes, *Science*, 2006, **311**, 832-835.
47. D. Laage and J. T. Hynes, *J. Phys. Chem. B*, 2008, **112**, 14230-14242.
48. D. Laage, G. Stirnemann, F. Sterpone, R. Rey and J. T. Hynes, *Annu. Rev. Phys. Chem.*, 2011, **62**, 395-416.
49. F. Sterpone, G. Stirnemann and D. Laage, *J. Am. Chem. Soc.*, 2012, **134**, 4116-4119.
50. D. Laage, G. Stirnemann and J. T. Hynes, *J. Phys. Chem. B*, 2009, **113**, 2428-2435.
51. J. Boisson, G. Stirnemann, D. Laage and J. T. Hynes, *Phys. Chem. Chem. Phys.*, 2011, **13**, 19895-19901.
52. G. Stirnemann, E. Wernersson, P. Jungwirth and D. Laage, *J. Am. Chem. Soc.*, 2013, **135**, 11824-11831.
53. J. Chowdhary and B. M. Ladanyi, *J. Phys. Chem. A*, 2011, **115**, 6306-6316.
54. L. Martínez, R. Andrade, E. G. Birgin and J. M. Martínez, *J. Comput. Chem.*, 2009, **30**, 2157-2164.
55. H. J. C. Berendsen, J. R. Grigera and T. P. Straatsma, *J. Phys. Chem.*, 1987, **91**, 6269-6271.
56. W. L. Jorgensen, D. S. Maxwell and J. TiradoRives, *J. Am. Chem. Soc.*, 1996, **118**, 11225-11236.
57. K. J. Schweighofer, U. Essmann and M. Berkowitz, *J. Phys. Chem. B*, 1997, **101**, 3793-3799.
58. H. Dominguez and M. L. Berkowitz, *J. Phys. Chem. B*, 2000, **104**, 5302-5308.
59. W. L. Jorgensen, J. Chandrasekhar, J. D. Madura, R. W. Impey and M. L. Klein, *J. Chem. Phys.*, 1983, **79**, 926-935.
60. E. Stewart, R. L. Shields and R. S. Taylor, *J. Phys. Chem. B*, 2003, **107**, 2333-2343.
61. C. D. Daub, K. Leung and A. Luzar, *J. Phys. Chem. B*, 2009, **113**, 7687-7700.
62. M. Chen, X. Lu, X. Liu, Q. Hou, Y. Zhu and H. Zhou, *Langmuir.*, 2014, **30**, 10600-10607.
63. B. Hess, H. Bekker, H. J. Berendsen and J. G. Fraaije, *J. Comput. Chem.*, 1997, **18**, 1463-1472.
64. T. Darden, D. York and L. Pedersen, *J. Chem. Phys.*, 1993, **98**, 10089.
65. U. Essmann, L. Perera, M. L. Berkowitz, T. Darden, H. Lee and L. G. Pedersen, *J. Chem. Phys.*, 1995, **103**, 8577-8593.

66. H. J. Berendsen, D. van der Spoel and R. van Drunen, *Comput. Phys. Commun.*, 1995, **91**, 43-56.
67. E. Lindahl, B. Hess and D. Van Der Spoel, *J. Mol. Model.*, 2001, **7**, 306-317.
68. D. Van Der Spoel, E. Lindahl, B. Hess, G. Groenhof, A. E. Mark and H. J. Berendsen, *J. Comput. Chem.*, 2005, **26**, 1701-1718.
69. B. Hess, C. Kutzner, D. Van Der Spoel and E. Lindahl, *J. Chem. Theory Comput.*, 2008, **4**, 435-447.
70. G. Bussi, D. Donadio and M. Parrinello, *J. Chem. Phys.*, 2007, **126**, 014101.
71. H. Martínez, E. Chacón, P. Tarazona and F. Bresme, *Proc. R. Soc. A*, 2011, **467**, 1939-1958.
72. M. Chen, X. Lu, X. Liu, Q. Hou, Y. Zhu and H. Zhou, *J. Phys. Chem. C*, 2014, **118**, 19205-19213.
73. D. E. Rosenfeld and C. A. Schmuttenmaer, *J. Phys. Chem. B*, 2010, **115**, 1021-1031.
74. N. Choudhury, *J. Chem. Phys.*, 2010, **133**, 154515.
75. N. Choudhury, *Chem. Phys.*, 2013, **421**, 68-76.
76. M. Sega, R. Vallauri and S. Melchionna, *Phys. Rev. E*, 2005, **72**, 041201.
77. S. Han, P. Kumar and H. E. Stanley, *Phys. Rev. E*, 2008, **77**, 030201.
78. N. Abrankó-Rideg, M. Darvas, G. Horvai and P. Jedlovsky, *J. Phys. Chem. B*, 2013, **117**, 8733-8746.
79. J. F. Kincaid, H. Eyring and A. E. Stearn, *Chem. Rev.*, 1941, **28**, 301-365.
80. J. W. Caldwell and P. A. Kollman, *J. Phys. Chem.*, 1995, **99**, 6208-6219.
81. G. Lamoureux, A. D. MacKerell Jr and B. Roux, *J. Chem. Phys.*, 2003, **119**, 5185-5197.
82. E. Wernersson and P. Jungwirth, *J. Chem. Theory Comput.*, 2010, **6**, 3233-3240.

Table of Content



Macroscopic polarization effect and retardation of ions and ionic groups concertedly lead to water dynamics slowdown in Newton black films.